Phase diagrams and thermochemical modeling of salt lake brine systems. III. $Li_2SO_4 + H_2O$, $Na_2SO_4 + H_2O$, $K_2SO_4 + H_2O$, $MgSO_4 + H_2O$ and $CaSO_4 + H_2O$ systems

Dongdong Li[a,b,*], Dewen Zeng[a,c,*], Xia Yin[d], Dandan Gao[a,e]

[a] Key Laboratory of Comprehensive and Highly Efficient Utilization of Salt Lake Resources, Qinghai Institute of Salt Lakes, Chinese Academy of Sciences, Xining 810008, PR China
[b] Key Laboratory of Salt Lake Resources Chemistry of Qinghai Province, Xining 810008, PR China
[c] College of Chemistry and Chemical Engineering, Central South University, Changsha 410083, PR China
[d] College of Chemistry and Chemical Engineering, Hunan University, Changsha 410082, PR China
[e] Qinghai Engineering and Technology Research Center of Comprehensive Utilization of Salt Lake Resources, Xining 810008, PR China

ARTICLE INFO

ABSTRACT

This paper is part of a series of studies on the development of a multi-temperature thermodynamically consistent model for salt lake brine systems. Under the comprehensive thermodynamic framework proposed in our previous study, the thermodynamic and phase equilibria properties of the sulfate binary systems (i.e., Li_2SO_4 + H_2O, Na_2SO_4 + H_2O, K_2SO_4 + H_2O, $MgSO_4$ + H_2O and $CaSO_4$ + H_2O) were simulated using the Pitzer-Simonson-Clegg (PSC) model. Various type of thermodynamic properties (i.e., water activity, osmotic coefficient, mean ionic activity coefficient, enthalpy of dilution and solution, relative apparent molar enthalpy, heat capacity of aqueous phase and solid phases) were collected and fitted to the model equations. The thermodynamic properties of these systems can be well reproduced or predicted using the obtained model parameters. Comparisons with the experimental or model values in literature indicate that the model parameters determined in this study can describe all of the thermodynamic and phase equilibria properties of these binary sulfate systems from infinite dilution to saturation and freezing point temperature to approx. 500 K.

1. Introduction

Thermodynamic modeling of phase diagrams is of essential importance for revealing the natural brine evolution and designing chemical engineering process to extract valuable salts from salt lake brines by predicting their salt formation sequence. In previous studies [1,2], the Pitzer-Simonson-Clegg (PSC) model [3,4] was chosen to represent the aqueous properties of binary salt-water systems (i.e. $LiCl + H_2O$, $NaCl + H_2O$, $KCl + H_2O$, $MgCl_2 + H_2O$ and $CaCl_2 + H_2O$). To regress the model parameters as a function of temperature, various type of thermodynamic data (i.e., water activity a_w, ionic activity coefficients $\gamma_{\pm}$, heat capacity of solution and solid phases c_p, enthalpy of dilution $\Delta_{dil}H_m$, enthalpy of solution $\Delta_{sol}H_m$, relative apparent molar enthalpy $^{\phi}L_m$ and solubility) were used as constraint conditions to guarantee parameters reliability. In recent years, the importance of thermodynamic constraints among different types of thermodynamic property for activity coefficient model parameterization has been noted and

valued by more and more researchers [5,6]. Emphasis was placed on the key role of the thermal quantities of the solid phases and the aqueous phase by the authors in the model parameterization under multi-temperature conditions. Under the parameterization framework, phase diagrams and thermodynamic properties of the binary systems $LiCl + H_2O$, $NaCl + H_2O$, $KCl + H_2O$, $MgCl_2 + H_2O$ and $CaCl_2 + H_2O$ were simulated in wide temperature and salt concentration ranges. To expand the modeling work for binary systems, which are the most important basis for the properties simulation and prediction of multi-component salt lake brine systems, herein binary sulfate systems $Li_2SO_4 + H_2O$, $Na_2SO_4 + H_2O$, $K_2SO_4 + H_2O$, $MgSO_4 + H_2O$ and $CaSO_4 + H_2O$ involved in the salt lake brine system are modeled using our previous proposed thermodynamic framework [1,2] to assure the compatibility in the multi-component system modeling, although these systems have been simulated by many other researchers [6–15] either with simple solubility models or comprehensive thermodynamic consistency models.

Table 1

Sources of experimental data used for parameterization of the binary systems $Li_2SO_4 + H_2O$, $Na_2SO_4 + H_2O$, $K_2SO_4 + H_2O$, $MgSO_4 + H_2O$ and $CaSO_4 + H_2O$.

System	Data Property[a]	Number of data points	Temperature Range/K	Concentration Range/mol·kg^{-1}	Reference
$Li_2SO_4 + H_2O$	Activity	99	383 − 498	0.54 − 3.18	[8]
	Activity	28	298.15	0.1 − 3.0	[21]
	Activity	120	298 − 323	0.1 − 2.8	[22]
	Activity	6	273.15	0.4 − 2.3	[23]
	Activity	7	323.15	0.75 − 3.1	[24]
	Activity	29	313.15	0.1 − 2.68	[25]
	Activity	17	298.15	0.7 − 2.87	[26]
	Thermal	10	303.15	0.17 − 0.92	[27]
	Thermal	19	298.15	0.15 − 3.0	[28]
	Thermal	10	298.15	0.0002 − 0.1	[29]
	SLE	11	251 − 487	0.38 − 3.38	[30]
	SLE	4	368 − 377	2.78 − 2.80	[31]
	SLE	4	253 − 323	2.97 − 3.40	[32]
	SLE	6	282 − 323	3.0 − 3.2	[33]
	SLE	1	298.15	3.16	[34]
	SLE	1	303.15	3.09	[35]
	SLE	19	257 − 376	2.83 − 3.42	[36]
	SLE	4	273 − 348	2.9 − 3.3	[37]
	SLE	7	258 − 373	2.79 − 3.36	[38]
$Na_2SO_4 + H_2O$	Activity	80	383 − 498	0.55 − 3.42	[8]
	Activity	11	273.15	0.1 − 1.5	[40]
	Activity	96	298 − 323	0.1 − 3.73	[41]
	Activity	25	323 − 423	0.47 − 1.85	[42]
	Activity	13	318.15	0.7 − 3.5	[43]
	Activity	13	333.15	0.9 − 3.44	[44]
	Activity	30	353.15	0.7 − 2.97	[45]
	Activity	10	372.75	0.9 − 3.5	[46]
	Activity	6	298.15	0.5 − 3.0	[47]
	Activity	64	298.15	0.001 − 1.95	[48]
	Activity	6	298.15	0.05 − 1.0	[49]
	Thermal	6	303.15	0.18 − 1.0	[27]
	Thermal	14	298.15	0.25 − 3.0	[28]
	Thermal	20	313 − 353	0.07 − 1.6	[50]
	Thermal	25	373 − 423	0.02 − 2.14	[51]
	Thermal	9	298.15	0.05 − 1.27	[52]
	Thermal	11	298.15	0.01 − 1.5	[53]
	Thermal	34	304 − 413	0.05 − 2.63	[54]
	SLE	25	308 − 514	2.94 − 3.46	[39]
	SLE	11	330 − 371	3.03 − 3.60	[55]
	SLE	12	272 − 303	0.28 − 2.82	[58]
	SLE	16	298 − 303	1.95 − 2.98	[59]
	SLE	14	273 − 305	0.33 − 3.78	[60]
	SLE	5	288 − 298	0.91 − 1.93	[61]
	SLE	6	273 − 297	1.25 − 3.69	[62]
	SLE	2	313 − 323	3.26 − 3.38	[63]
$K_2SO_4 + H_2O$	Activity	55	383 − 498	0.55 − 2.71	[8]
	Activity	53	298 − 323	0.2 − 0.96	[10]
	Activity	74	273 − 498	0.1 − 2.5	[10] [b]
	Activity	7	298.15	0.1 − 0.7	[21]
	Activity	50	298.15	0.001 − 0.6	[43]
	Activity	42	298.15	0.001 − 0.05	[64]
	Thermal	4	303.15	0.12 − 0.56	[27]
	Thermal	19	373 − 423	0.0025 − 0.65	[51]
	Thermal	9	298.15	0.06 − 0.65	[52]
	Thermal	8	298.15	0.01 − 0.65	[53]
	Thermal	22	298 − 373	0.03 − 0.4	[65]
	SLE	56	271.6 − 562.15	0.402 − 2.06	[66]
$MgSO_4 + H_2O$	Activity	14	273.15	0.005 − 5.65	[40]
	Activity	6	372.75	2.0 − 4.5	[46]
	Activity	3	298.15	1.0 − 3.0	[47]
	Activity	30	273.15 − 373.15	0.72 − 5.65	[67]
	Activity	14	288.15	0.1 − 3.0	[68]
	Activity	48	298.15	0.1 − 3.6176	[69]
	Activity	17	298.15	0.1 − 3.0	[70]
	Activity	10	298.15	0.933 − 3.485	[71]
	Activity	9	298.15	1.48 − 2.98	[72]
	Activity	36	383.15 − 413.22	1.38 − 5.05	[73]
	Activity	13	298.15	0.005 − 0.149	[74]
	Thermal	6	303.15	0.341 − 1.059	[27]
	Thermal	16	313.15 − 353.15	0.1 − 1.968	[50]
	Thermal	30	373.15 − 423.65	0.002 − 2.712	[51]
	Thermal	41	348.15 − 473.15	0.1 − 2.186	[75]
	SLE	8	269.28 − 272.85	1.6739 − 2.1043	[76]
	SLE	32	273.15 − 363.15	2.195 − 5.732	[77]

Table 1 (continued)

System	Data Property[a]	Number of data points	Temperature Range/K	Concentration Range/mol·kg^{-1}	Reference
	SLE	6	303.04 – 318.16	3.234 – 3.956	[78]
	SLE	52	348.15 – 511.15	0.047 – 6.198	[79]
	SLE	14	333.45 – 368.55	4.236 – 5.929	[80]
CaSO$_4$ + H$_2$O	Activity	20	298.15	0.0002 – 0.01273	[64]
	Activity	7	298.15	0.0006 – 0.01518	[81]
	Thermal	8	298.15	0.00004 – 0.0016	[29]
	SLE	11	298.15 – 373.15	0.005 – 0.0202	[82]
	SLE	2	323.15 – 348.15	0.0077 – 0.0141	[83]
	SLE	4	318.15 – 338.15	0.01 – 0.0155	[84]
	SLE	98	371.65 – 493.15	0.0004 – 0.01257	[85]
	SLE	12	273.65 – 383.15	0.01 – 0.0158	[86]

[a] Activity stands for water activity, osmotic coefficient and mean ionic activity coefficient; Thermal stands for enthalpy of dilution, enthalpy of solution, relative apparent molar enthalpy, specific heat and apparent molar heat capacity; SLE stands for solid-liquid equilibria data.

[b] Model generated values of osmotic coefficient and mean ionic activity coefficient in literature [10] (see Table 7 and 8 in literature [10]).

Table 2

Assessed temperature-dependent PSC model parameters for Li$_2$SO$_4$(aq), Na$_2$SO$_4$(aq), K$_2$SO$_4$(aq), MgSO$_4$(aq) and CaSO$_4$(aq) solution.

Parameter[a]	$P(T) = a_0 + a_1 T + a_2 T \ln(T) + a_3 T^2 + a_4 T^3 + a_5/T$					
	a_0	a_1	a_2	a_3	a_4	a_5
$B_{Li2SO4(aq)}$	−5.6319170084E+05	1.2703594817E+04	−2.1191781722E+03	3.5004648322E+00	−1.0730195382E−03	2.7684396488E+07
$B^1_{Li2SO4(aq)}$	0	0	0	0	0	0
$W_{1,Li2SO4(aq)}$	−3.4984894159E+05	7.3876502325E+03	−1.2137745463E+03	1.8048488890E+00	−4.8216277978E−04	1.8315189322E+07
$U_{1,Li2SO4(aq)}$	−8.9026767290E+05	1.8988999613E+04	−3.1273007648E+03	4.7308988738E+00	−1.2952411112E−03	4.6188532998E+07
$V_{1,Li2SO4(aq)}$	6.5208216489E+05	−1.4049953002E+04	2.3194137856E+03	−3.5686719353E+00	1.0000841369E−03	−3.3519285537E+07
$B_{Na2SO4(aq)}$	4.2917241284E+05	−1.3007475227E+04	2.2941659328E+03	−5.1432636824E+00	2.0770595704E−03	−1.3705307349E+07
$B^1_{Na2SO4(aq)}$	0	0	0	0	0	0
$W_{1,Na2SO4(aq)}$	−2.4170669327E+05	4.3922102430E+03	−6.9336722292E+02	7.1698067936E−01	−6.0149268162E−05	1.4274494838E+07
$U_{1,Na2SO4(aq)}$	−6.1758814707E+05	1.1782875969E+04	−1.8860208952E+03	2.2490235140E+00	−3.6623771410E−04	3.5228682375E+07
$V_{1,Na2SO4(aq)}$	3.5514905614E+05	−6.1204593033E+03	9.5090888420E+02	−8.0804986946E−01	−3.5911885424E−05	−2.1736481776E+07
$B_{K2SO4(aq)}$	3.2780024818E+05	−7.9418920863E+03	1.3450852249E+03	−2.4359347597E+00	8.1991908857E−04	−1.4939774543E+07
$B^1_{Na2SO4(aq)}$	0	0	0	0	0	0
$W_{1,Na2SO4(aq)}$	−4.8460772325E+04	1.1392720645E+03	−1.9191131596E+02	3.3784232066E−01	−1.1125862677E−04	2.3006130118E+06
$U_{1,Na2SO4(aq)}$	−6.1798851141E+04	1.4648402067E+03	−2.4709452233E+02	4.3797844539E−01	−1.4486902263E−04	2.8977003079E+06
$V_{1,K2SO4(aq)}$	0	0	0	0	0	0
$B_{MgSO4(aq)}$	1.1138153352E+05	−3.1645936452E+03	5.5802456248E+02	−1.3079323076E+00	5.9119367146E−04	−4.4762717413E+06
$B^1_{MgSO4(aq)}$	7.3302760473E+05	−3.6266217541E+03	7.6553040657E+00	7.6110991193E+00	−6.3365700168E−03	−6.5719046485E+07
$W_{1,MgSO4(aq)}$	4.8580096056E+06	−1.2485149931E+05	2.1425316382E+04	−4.2160841231E+01	1.5611754117E−02	−2.0735531747E+08
$U_{1,MgSO4(aq)}$	1.0232647098E+07	−2.6305066655E+05	4.5147010033E+04	−8.8938036869E+01	3.2990219357E−02	−4.3688399212E+08
$V_{1,MgSO4(aq)}$	−5.3844618297E+06	1.3848367771E+05	−2.3772114941E+04	4.6898979482E+01	−1.7434935200E−02	2.2992097839E+08
$BCaSO4(aq)$	1.5213734011E+03	0	0	0	0	−3.7201570715E+05
$B^1_{CaSO4(aq)}$	3.2651574750E+04	0	0	0	0	−1.2220623741E+07
$W_{1,CaSO4(aq)}$	0	0	0	0	0	0
$U_{1,CaSO4(aq)}$	0	0	0	0	0	0
$V_{1,CaSO4(aq)}$	0	0	0	0	0	0

[a] All of the parameters can be found in Eq. (1) to (6) in ref [1]; for Li$_2$SO$_4$(aq) and K$_2$SO$_4$(aq), $\alpha = 13.0$, $\alpha_1 = 0.0$, for Na$_2$SO$_4$(aq), $\alpha = 2.0$ and $\alpha_1 = 0.0$ and for MgSO$_4$(aq) and CaSO$_4$(aq), $\alpha = 7.0$ and $\alpha_1 = 95.0$.

2. Thermodynamic framework and parameter regression method

The thermodynamic framework, parameter regression and data weighting method were performed according to our previous study [1,2] and not repeated here. For each binary system, the model parameters are also regressed with the PSCBREG program [1]. All of the collected experimental data respectively for a binary system are processed using PSCBREG in one simultaneous weighted least square regression.

For any species in an aqueous solution and any solid phase, its standard Gibbs energy as a function of temperature can be written as shown in Eq. (1).

$$G_i^\Theta(t) = A(t - t \ln t) - Bt^2/2 - Ct^3/6 - Dt^4/12 - E/2t + F - Gt \quad (1)$$

with $t = (T/K)/1000$ and T is the absolute temperature in Kelvin.

The standard enthalpy and entropy as well as the heat capacity can be derived from the fundamental thermodynamic relationships in Eqs. (2)–(4):

$$H_i^\Theta(t) = At + Bt^2/2 + Ct^3/3 + Dt^4/4 - E/t + F \quad (2)$$

$$S_i^\Theta(t) = A\ln t + Bt + Ct^2/2 + Dt^3/3 - E/2t^2 + G \quad (3)$$

$$C_{p,i}^\Theta(t) = A + Bt + Ct^2 + Dt^3 + E/t^2 \quad (4)$$

For all aqueous ion, its temperature coefficients (A, B, C, D and E) in Eqs. (1)–(4) are determined by fitting the individual isobaric heat capacity values calculated from the Helgeson-Kirkham-Flowers (HKF) equations of state (EOS) [16,17] that are incorporated into the CHNOSZ software package [18] over a temperature range of 273.15–523.15 K. The F and G coefficients in Eqs. (2) and (3) are evaluated by substituting $H_{i,298.15}^\Theta$ and $S_{i,298.15}^\Theta$ in the equations. The enthalpy and entropy values at 298.15 K are available in the same software package [18].

For an anhydrous salt solid whose heat capacity as a function of temperature is known, its A, B, C, D and E parameters can be read out directly from the NIST Webbook database [19]. For a hydrated salt solid whose heat capacity data are unavailable, their heat capacity $C_{p,MX·nH_2O_{(s)}}^\Theta(t)$ will be estimated using group contribution approaches:

Table 3

Standard Gibbs free energy as a function of temperature for the involved aqueous and solid species.

Aqueous species or minerals	$G_m^0(t) = A(t - tInt) - Bt^2/2 - Ct^3/6 - Dt^4/12 - E/2t + F - Gt$[a]							
	A	*B*	*C*	*D*	*E*	*F*	*G*	*T*/K
Li$^+$(aq)[b]	4908.41	−26562.4	54573.6	−40213.6	−63.4622	−1176.824	11443.528	273–523
Na$^+$(aq)[b]	8348.7	−42244.5	80859.5	−55349.6	−127.822	−1885.564	18932.935	273−523
K$^+$(aq)[b]	5097.33	−25943.2	49804.1	−34187.3	−77.8793	−1252.516	11654.894	273−523
Mg^{2+}(aq)[b]	6638.14	−37893.1	79861.3	−60195.6	−83.0268	−1625.991	15708.155	273−523
Ca^{2+}(aq)[b]	14540.6	−77281.2	154173	−110453	−205.156	−3275.405	33550.695	273−523
SO$_4^{2-}$(aq)[c]	71423.6	−376630	744740	−526786	−1034.99	−14474.708	164476.054	273−523
H$_2$O(l)[b]	−90.0669	748.166	−1377.94	1055.31	3.26118	−271.203	−191.886	180−523
H$_2$O(cr, I)[b]	13.44	20.2535	371.643	−418.377	−0.0301987	−300.209	42.01	100−273
Li$_2$SO$_4$·H$_2$O(cr)[d]	173.9203	25.1140	104.2193	−33.7087	−2.5501	−1796.0145	350.0485	253−523
Na$_2$SO$_4$·10H$_2$O(cr)[e]	531.9747	149.5454	−44.5116	14.2431	−0.8749	−4494.6767	1191.6295	252−273
Na$_2$SO$_4$·7H$_2$O(cr)[e]	356.8389	149.5454	−44.5116	14.2431	−0.8749	−3551.4221	868.8610	240−256
Na$_2$SO$_4$(cr, V)[e]	96.9747	149.5454	−44.5116	14.2431	−0.8749	−1426.4541	217.6080	263−453
K$_2$SO$_4$(cr)[e]	139.5050	−1.1999	136.8080	−47.1432	−1.6640	−1486.2538	328.9267	273−500
MgSO$_4$·11H$_2$O(cr)[e]	554.3321	111.7220	−39.6884	5.1298	−0.8326	−4738.5320	1157.8261	269−273
MgSO$_4$·7H$_2$O(cr)[e]	380.3321	111.7220	−39.6884	5.1298	−0.8326	−3511.2992	782.4061	285−318
MgSO$_4$·6H$_2$O(cr)[e]	336.8321	111.7220	−39.6884	5.1298	−0.8326	−3195.2631	712.4415	273−373
MgSO$_4$·5H$_2$O(cr)[e]	293.3321	111.7220	−39.6884	5.1298	−0.8326	−2885.7932	618.1410	358−373
MgSO$_4$·4H$_2$O(cr)[e]	249.8321	111.7220	−39.6884	5.1298	−0.8326	−2579.8885	512.4496	358−373
MgSO$_4$·H$_2$O(cr)[e]	119.3321	111.7220	−39.6884	5.1298	−0.8326	−1657.0038	217.6485	348−510
CaSO$_4$·2H$_2$O(cr)[e]	155.7731	201.6780	−194.4670	85.3175	−1.1345	−2090.1013	292.4367	273−383
CaSO$_4$·1/2H$_2$O(cr)[e]	90.5231	201.6780	−194.4670	85.3175	−1.1345	−1623.8919	154.9362	371−473
CaSO$_4$(cr)[e]	68.7731	201.6780	−194.4670	85.3175	−1.1345	−1475.7219	100.6272	298−393

[a] $t = (T/K)/1000$.

[b] According to our previous study [1,2].

[c] Determined by fitting the thermodynamic values calculated from the HKF equation of state [16,17] using the CHNOSZ software package [18].

[d] Parameters *A*, *B*, *C*, *D* and *E* were taken from the NIST WebBook [19], and *F* and *G* were determined by fitting to experimental solubility data.

[e] Parameters *A*, *B*, *C*, *D* and *E* were estimated using Eq. (5), and *F* and *G* were determined by fitting to experimental solubility data.
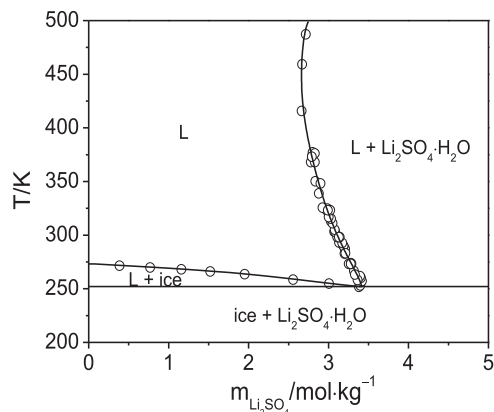

Fig. 1. Phase diagram of the Li$_2$SO$_4$ + H$_2$O system. Symbols: experimental data reported in literature [30–38]. Lines: the present model results.

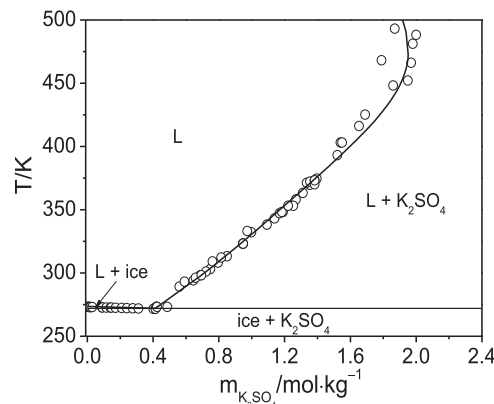**Fig. 2.** Phase diagram of the Na$_2$SO$_4$ + H$_2$O system. Symbols: experimental data reported in literature [39,55–63]. Lines: the present model results.

Fig. 3. Phase diagram of the K$_2$SO$_4$ + H$_2$O system. Symbols: experimental data reported in literature [66]. Lines: the present model results.
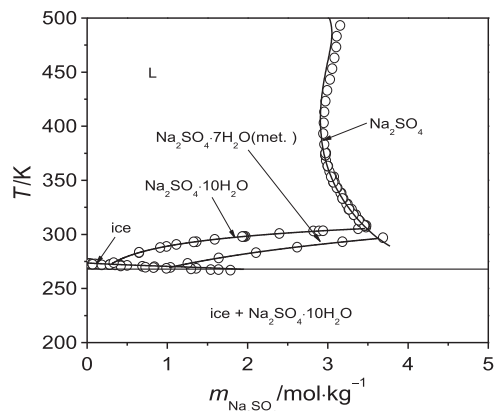

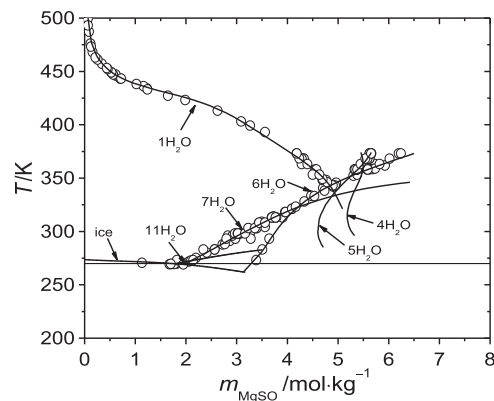**Fig. 4.** Phase diagram of the MgSO$_4$ + H$_2$O system. Symbols: experimental data reported in literature [39,76–80]. Lines: the present model results.

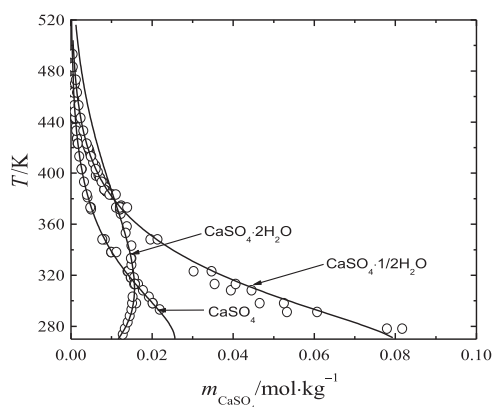**Fig. 5.** Phase diagram of the $CaSO_4 + H_2O$ system. Symbols: experimental data reported in literature [82–86]. Lines: the present model results.

$$C_{p,MX \cdot nH_2O_{(s)}}^{\Theta}(t) = C_{p,MX_{(s)}}^{\Theta}(t) + nC_{p,H_2O}^{\Theta} \quad (5)$$

where $C_{p,MX \cdot nH_2O_{(s)}}^{\Theta}(t)$ and $C_{p,MX_{(s)}}^{\Theta}(t)$ are the heat capacity of the hydrated and anhydrous salt at temperature t, respectively, and C_{p,H_2O}^{Θ} is the group contribution of one crystal water molecule to the heat capacity of the hydrated salt independent of temperature and set to 43.5 $J \cdot K^{-1} \cdot mol^{-1}$, as recommended by Archer [20].

The rest of parameters (F and G) of a solid phase will be evaluated by fitting to the solubility data at various temperatures.

3. Determination of model parameters

The model parameters for the binary systems $Li_2SO_4 + H_2O$, $Na_2SO_4 + H_2O$, $K_2SO_4 + H_2O$, $MgSO_4 + H_2O$ and $CaSO_4 + H_2O$ were determined using various types of thermodynamic data including the water activity a_w and osmotic coefficient ϕ, mean ionic activity coefficient $\gamma_{\pm}$, enthalpy of dilution $\Delta_{dil}H_m$ or solution $\Delta_{sol}H_m$, relative apparent molar enthalpy $^{\phi}L_m$, heat capacity c_p and solid-liquid equilibria

data. All of the data were available in the literature [8,10,21–86] and summarized in Table 1. Among these data, the model correlated values in comprehensive reviews [7,10,39,41,71], the solubility data of ice or the freezing points and some thermal data with large uncertainty are cited for comparison to the present model results rather than for regressing the model parameters. These experimental data along with their assigned weight factors used for parameter determination are collected in Appendix A. For the studied systems, the collected experimental data covers a temperature range from freezing point to approx. 500 K. Even though sometime the model can be used to represent the solubility data at higher temperatures, the solubility data at too high temperature were excluded considering the limitation of the thermodynamic properties of the corresponded aqueous solutions. The assessment procedure for the weight factors was described in our previous study detailed [1].

The regressed model parameters for the five binary sulfate systems are listed in Tables 2 and 3, respectively. Table 2 lists the PSC model parameters as a function of temperature. Table 3 lists the temperature coefficients of standard state properties for all aqueous and solid species that were included in the present models. All of the coefficients for the ions were fitted to the values calculated from the HKF equations [16,17] that were incorporated in the CHNOSZ software package [18], the coefficients A, B, C, D, E for the solids were determined from their heat capacities at various temperatures and F and G were determined by fitting to the solubility data.

4. Results and discussion

4.1. Phase diagrams and invariant points

The model calculated phase diagrams of the $Li_2SO_4 + H_2O$, $Na_2SO_4 + H_2O$, $K_2SO_4 + H_2O$, $MgSO_4 + H_2O$ and $CaSO_4 + H_2O$ systems compared with solubility data reported in literature [30–39,55–63,66,76–81,83–87] are plotted in Figs. 1–5. The predicted invariant points for these systems are listed in Table 4 and compared with the literature values [12,15,39,76,84,86,88].

As shown in Figs. 1–5 and Table 4, most of the solid-liquid equilibria

Table 4
Comparison of invariant points in the systems $Li_2SO_4 + H_2O$, $Na_2SO_4 + H_2O$, $K_2SO_4 + H_2O$, $MgSO_4 + H_2O$ and $CaSO_4 + H_2O$.

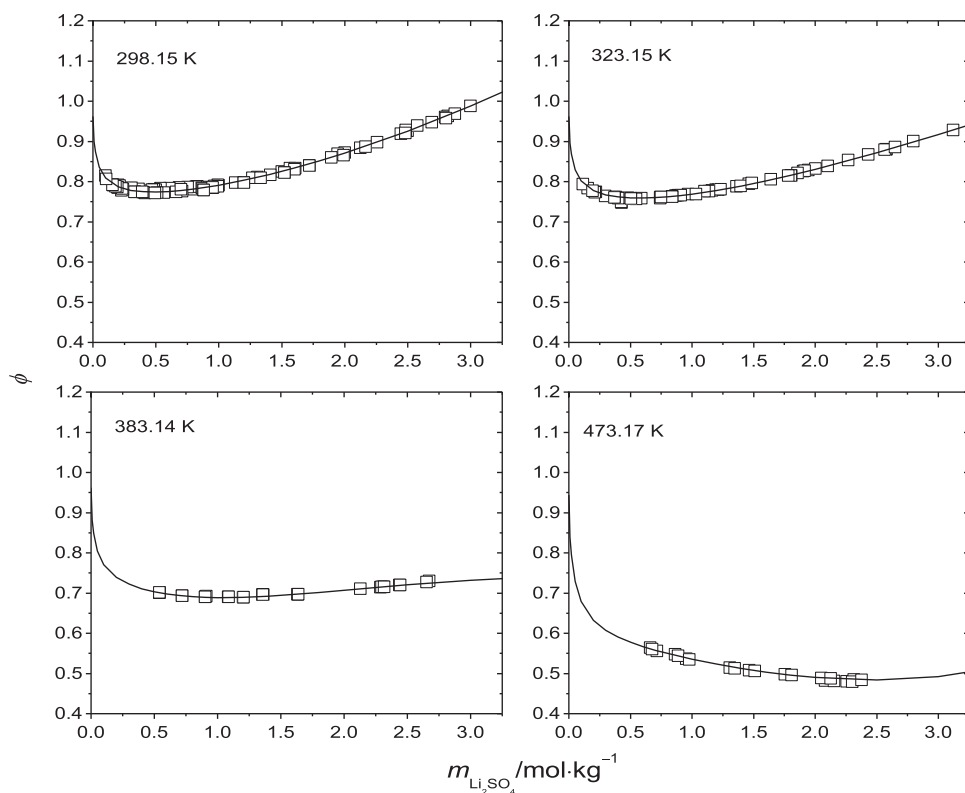| Invariant point	Type[a]	Transition temperature/K	Composition/(100w)	Composition/(mol·kg⁻¹ H₂O)	Reference
Ice + Li₂SO₄·H₂O	E	252.23	27.30	3.415	This work
		250.15	27.90	3.519	[39]
		250.6 ± 2.0	27.56 ± 0.55	3.460 ± 0.05	[87]
Ice + Na₂SO₄·10H₂O	E	272.62	4.10	0.301	This work
		272.01	4.02	0.295	[12]
		271.99	4.03	0.296	[88]
Na₂SO₄·10H₂O + Na₂SO₄(V)	P	305.42	33.10	3.483	This work
		305.55	33.20	3.499	[39]
		305.53	33.24	3.505	[12]
Ice + K₂SO₄	E	272.06	6.69	0.411	This work
		271.25	7.29	0.451	[39]
		271.55	6.67	0.410	[88]
Ice + MgSO₄·11H₂O	E	269.85	17.53	1.766	This work
		269.45	17.40	1.750	[76]
		269.65	17.32	1.740	[88]
MgSO₄·11H₂O + MgSO₄·7H₂O	P	272.53	20.13	2.094	This work
		273.75	21.1	2.221	[76]
		273.76	20.8	2.182	[88]
MgSO₄·7H₂O + MgSO₄·6H₂O	P	322.64	33.58	4.200	This work
		321.15	33.0	4.092	[39]
MgSO₄·6H₂O + MgSO₄·H₂O	P	342.89	36.83	4.844	This work
		342.15	37.10	4.900	[39]
CaSO₄·2H₂O + CaSO₄	P	314.34	0.21	0.015	This work
		315.0	–	–	[15]
		~313.15	–	–	[85]
		315.15	–	–	[84]

[a] E: eutectic point; P: peritectic point.

Fig. 6. Osmotic coefficients ϕ of Li$_2$SO$_4$(aq) solution at various temperatures and molalities. Symbols: experimental data reported in literature [8,16,22,24,26]; Lines: the present model results.

data, i.e. the points on the solubility curve and the invariant points, can be reproduced well using the present comprehensive thermodynamic models. Ice solubility data for all of these systems can be accurately predicted even though they were not used in model parameterization.

The solubility data of solid phase Li$_2$SO$_4$·2H$_2$O(cr) that listed but questioned in the compilation of Linke [39] were not included in the

present model. The available solubility data of K$_2$SO$_4$ above 420 K are scattered and hard to give a critical evaluation on their reliability, therefore these data were all used in parameterization. Nevertheless, the model result was not affected by the scattered experimental data significantly in the temperature range from 420 K to 500 K, but gave a regular variation. In the systems Na$_2$SO$_4$+H$_2$O, MgSO$_4$+H$_2$O and
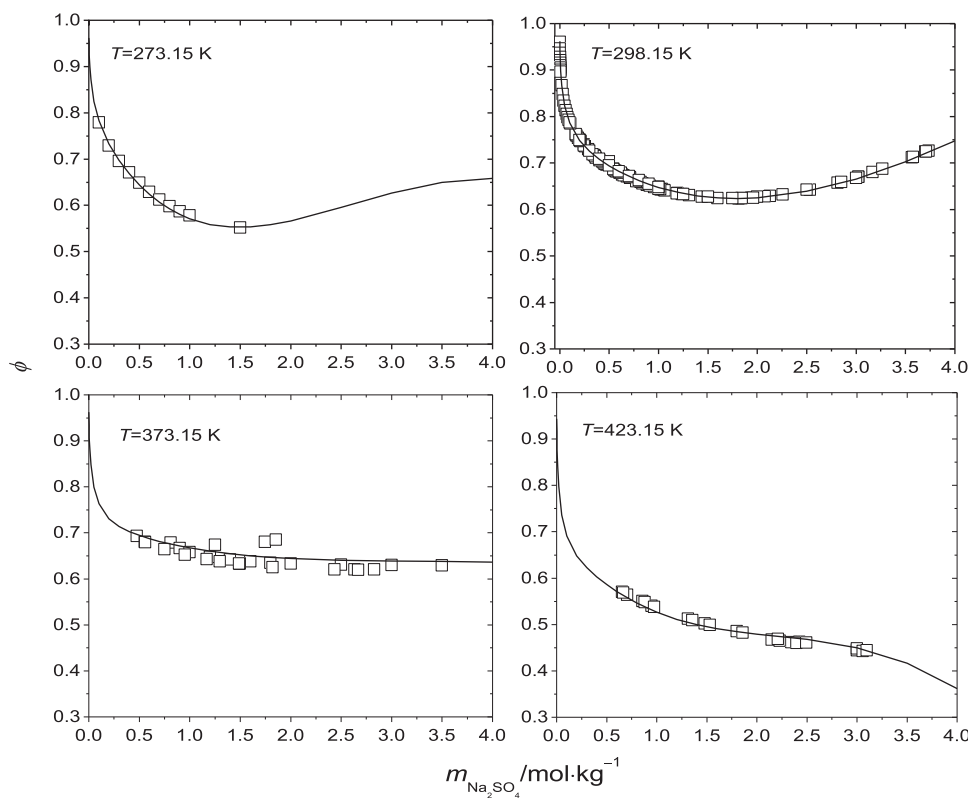
Fig. 7. Osmotic coefficients ϕ of Na$_2$SO$_4$(aq) solution at various temperatures and molalities. Symbols: experimental data in literature [8,40–42,46,48]; Lines: the present model results.
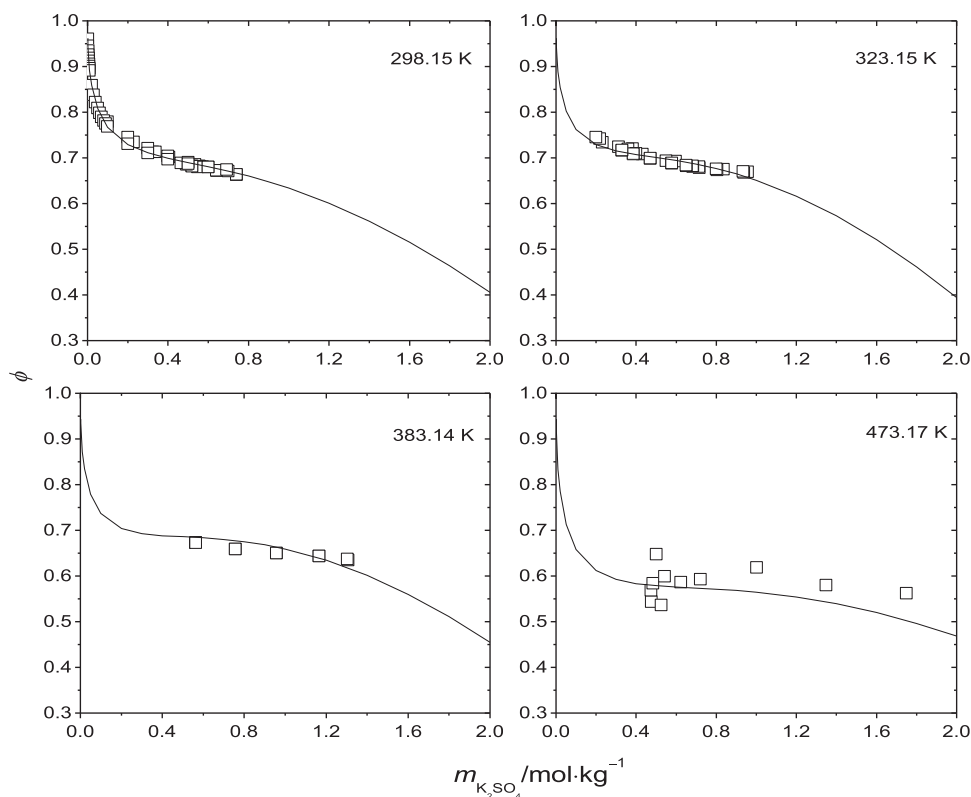
Fig. 8. Osmotic coefficients ϕ of K$_2$SO$_4$(aq) solution at various temperatures and molalities. Symbols: experimental data reported in literature [8,10,21,46,48]; Lines: the present model results.

CaSO$_4$+H$_2$O, the solubilities of metastable solid phases Na$_2$SO$_4$·7H$_2$O (cr), MgSO$_4$·4H$_2$O(cr), MgSO$_4$·5H$_2$O(cr) and CaSO$_4$·1/2H$_2$O(cr) were also simulated except for those stable solid phases. MgSO$_4$·11H$_2$O(cr) [12,89,90] was recognized as stable phase at low temperature, although the solid phase corresponding to its solubilities in early literature were determined as MgSO$_4$·12H$_2$O [76,88].

The difference of eutectic temperature of Li$_2$SO$_4$·H$_2$O + ice between the present model predicted value and that recommended by Linke [39] and Sohr et al. [87] is about 2 K. According to the critical evaluation of Sohr et al., the uncertainty of the eutectic temperature is 2 K. So in such a uncertainty range, the present model result agrees with the recent recommendation of Sohr et al. [87] well. The eutectic composition of
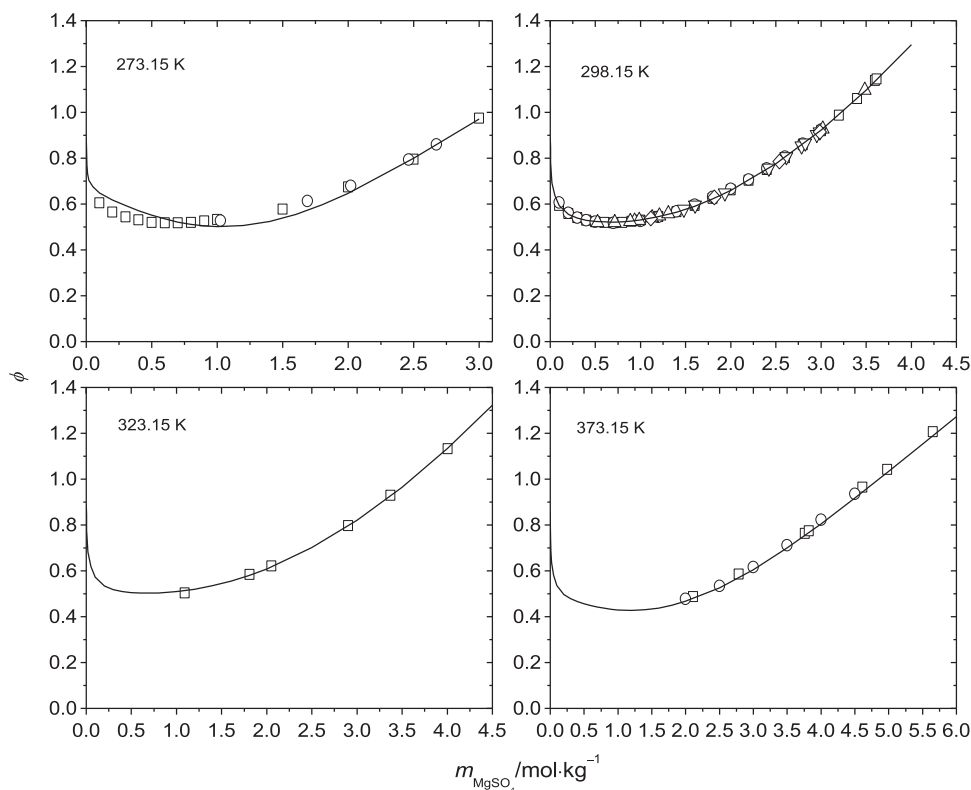

Fig. 9. Osmotic coefficients ϕ of MgSO$_4$(aq) solution at various temperatures and molalities. Symbols: experimental data reported in literature [40,67,69–72]; Lines: the present model results.
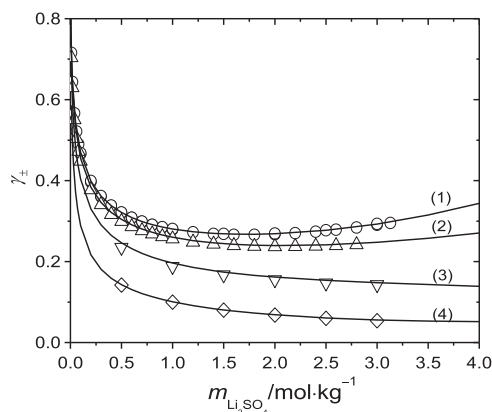
Fig. 10. Mean ionic activity coefficient $\gamma_\pm$ of Li_2SO_4(aq) solution at various molalities and (1) $T = 298.15$ K, (2) $T = 323.15$ K, (3) $T = 383.15$ K and (4) $T = 473.15$ K. Symbols: literature values [21,22]; Lines: the present model results.
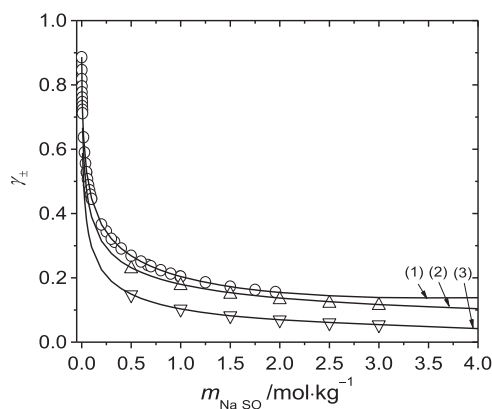

Fig. 11. Mean ionic activity coefficient $\gamma_\pm$ of Na_2SO_4(aq) solution at various molalities and (1) $T = 298.15$ K, (2) $T = 383.15$ K and (3) $T = 473.15$ K. Symbols: literature values [8,48]; Lines: the present model results.

this invariant point predicted from the present model agree with those reported by Linke [39] and Sohr et al. [87] in absolute error 0.6% weight percentage, which is in accordance with the uncertainty reported by Sohr et al. [87] recently.

For the invariant points in the systems $Na_2SO_4 + H_2O$, $K_2SO_4 + H_2O$, $MgSO_4 + H_2O$ and $CaSO_4 + H_2O$, the difference between the present model results and literature values is within 1 K. The compositions (mass percent) of the invariant points predicted from the present
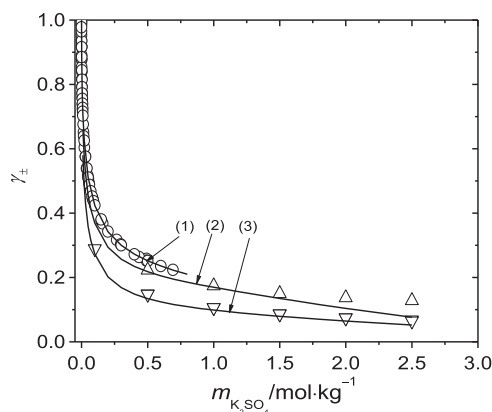

Fig. 12. Mean ionic activity coefficient $\gamma_\pm$ of K_2SO_4(aq) solution at various molalities and (1) $T = 298.15$ K, (2) $T = 383.15$ K and (3) $T = 473.15$ K. Symbols: literature values [10,48,64]; Lines: the present model results.
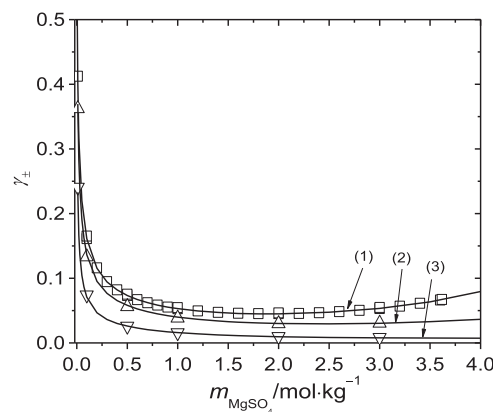

Fig. 13. Mean ionic activity coefficient $\gamma_\pm$ of $MgSO_4$(aq) solution at various molalities and (1) $T = 298.15$ K, (2) $T = 348.15$ K and (3) $T = 423.15$ K. Symbols: literature values [69,73]; Lines: the present model results.

models agree with those reported in literature in absolute error 0.5% weight percentage.

4.2. Component activity in the aqueous phases

Figs. 6–9 show the model calculated and experimental osmotic coefficient [8,10,21,22,24,26,40–42,46] of Li_2SO_4(aq), Na_2SO_4(aq), K_2SO_4(aq) and $MgSO_4$(aq) solutions at various temperatures and molalities, indicating the present models can reproduce these experimental osmotic coefficient data, which equivalent to the activity of solvent water, well over wide temperature and concentration ranges. The present models can reproduce the mean ionic activity coefficients of these aqueous solutions at $T = 298.15$ K used for parameterization well and at the same time the predicted values at other temperature are also in agreement with other literature models values [8,10,22,73] as shown in Figs. 10–14 although those data were not used for parameter regression.

4.3. Thermal properties of aqueous phases

Figs. 15–17 show the enthalpy of dilution of Na_2SO_4(aq), K_2SO_4(aq) and $MgSO_4$(aq) solutions at various temperatures. The present models can reproduce those thermal data [27–29,50–54,65,75], which were used for model parameters regression. Fig. 18 shows the present model generated relative apparent molar enthalpies $^\phi L_m$ of Li_2SO_4(aq) solutions at various temperatures. The model values at $T = 298.15$ K are in good agreement with literature values [50]. Results at other higher
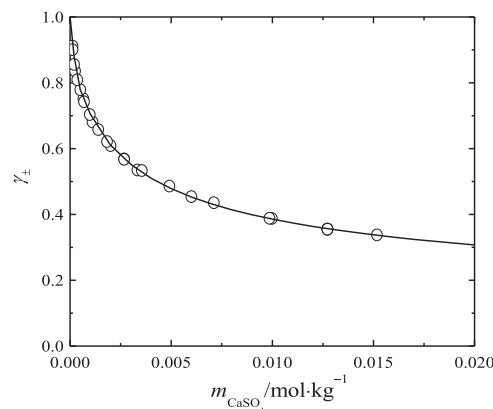

Fig. 14. Mean ionic activity coefficient $\gamma_\pm$ of $CaSO_4$(aq) solution at various molalities and $T = 298.15$ K. Symbols: literature values [64]; Lines: the present model results.

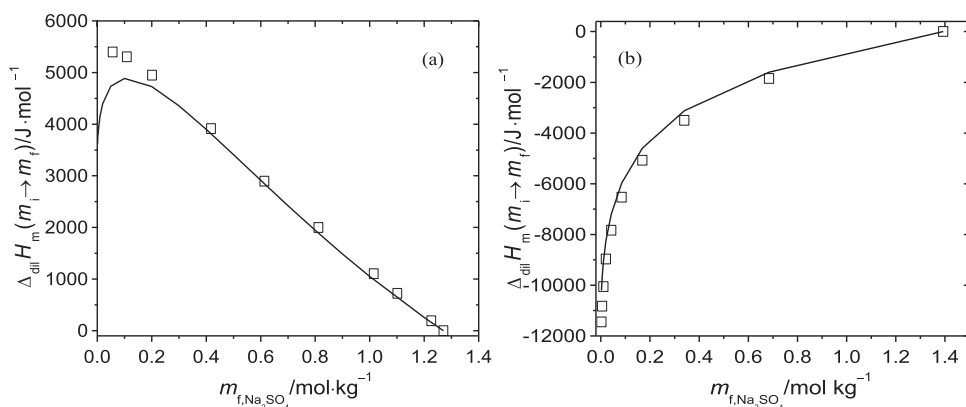**Fig. 15.** Enthalpy of dilution of Na$_2$SO$_4$(aq) solution at $T = 298.15$ K with initial molality $m_i = 1.2706$ mol·kg^{-1} (a) and $T = 373.15$ K with initial molality $m_i = 1.3930$ mol·kg^{-1} (b). Symbols: experimental data reported in literature [27,51]; Lines: the present model results.
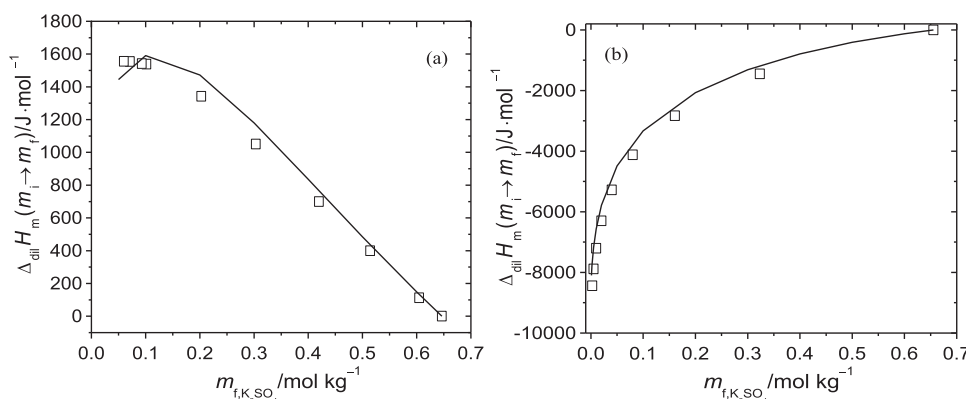
Fig. 16. Enthalpy of dilution of K$_2$SO$_4$(aq) solution at $T = 298.15$ K with initial molality $m_i = 0.6464$ mol·kg^{-1} (a) and $T = 373.15$ K with initial molality $m_i = 0.6553$ mol·kg^{-1} (b). Symbols: experimental data reported in literature [27,51]; Lines: the present model results.

Fig. 17. Enthalpy of dilution of MgSO$_4$(aq) solution at $T = 303.15$ K with initial molality $m_i = 1.05904$ mol·kg^{-1} (a) and $T = 373.15$ K with initial molality $m_i = 1.9880$ mol·kg^{-1} (b). Symbols: experimental data reported in literature [27,51]; Lines: the present model results.
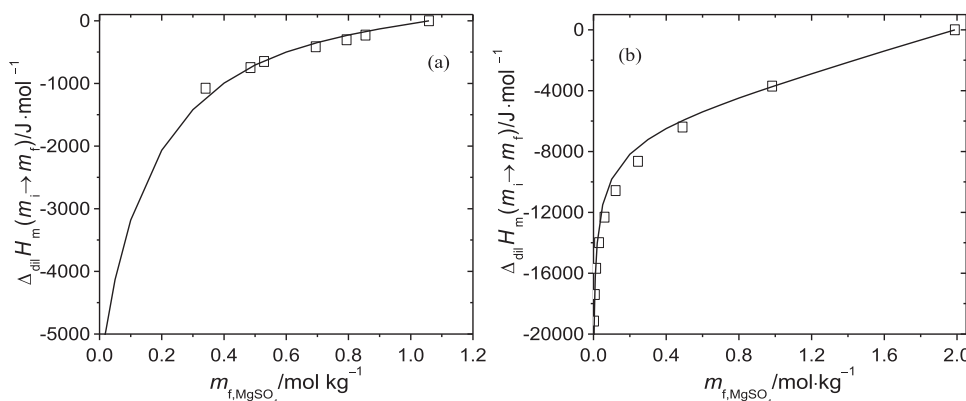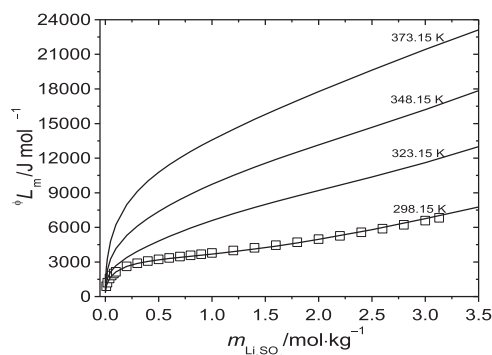

Fig. 18. Apparent relative molar enthalpy $^\phi L_m$ of Li$_2$SO$_4$(aq) solution at various temperatures and molalities. Symbols: experimental data reported in literature [50]; Lines: the present model results.

temperatures indicate that the $^\phi L_m$ of Li$_2$SO$_4$(aq) solution increased with temperature for a given concentration. Similar temperature behavior of the $^\phi L_m$ can also be found for CaSO$_4$(aq) solutions as shown in Fig. 19, although there is no experimental data existed to verify the correctness of those predicted values. Figs. 20–23 show the specific heat capacities of aqueous solutions at various temperatures and concentrations. For the system Li$_2$SO$_4$ + H$_2$O, those experimental heat capacity data [91,92] plotted in Fig. 20 were not used for parameterization due to the obvious scattered [91] and late publication [92] but well predicted by the present model, indicating the strong predictability of the model obtained from multi-property regression. For the systems Na$_2$SO$_4$ + H$_2$O, K$_2$SO$_4$ + H$_2$O and MgSO$_4$ + H$_2$O, those experimental heat capacity data that plotted in Figs. 21–23 were included in model parameters regression due to their well reliability and accuracy and the present models can reproduce those data reasonably.
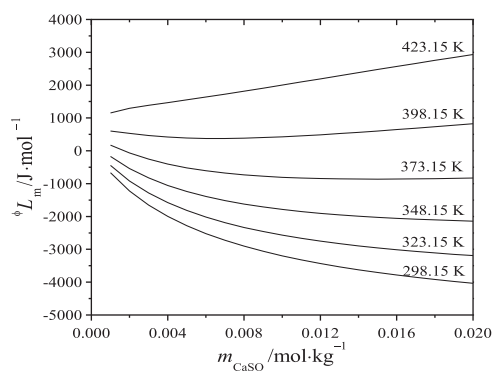
Fig. 19. Apparent relative molar enthalpy $^{\phi}L_{m}$ of $CaSO_4$(aq) solution at various temperatures and molalities. Lines: the present model results.
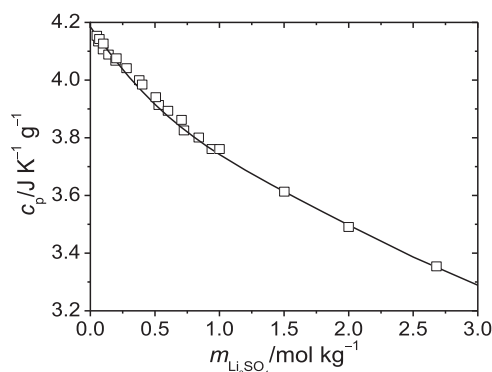

Fig. 20. Specific heat capacity c_p of Li_2SO_4(aq) solution at various molalities and $T = 298.15$ K. Symbols: experimental data reported in literature [91,92]; Lines: the present model results.

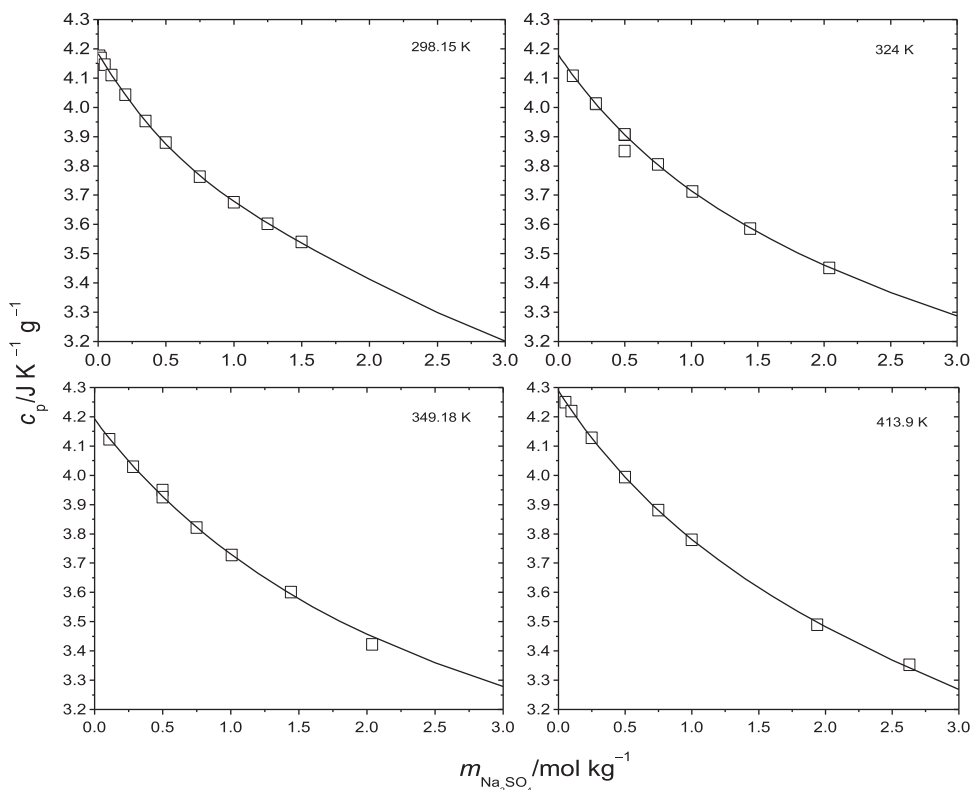### 4.4. Standard thermodynamic quantities of solid phases

The evaluated thermodynamic values of the solid phases in the five binary systems at standard state and 298.15 K are summarized in Table 5. The standard Gibbs energy $\Delta_f G_m^{\ominus}$ of $Li_2SO_4·H_2O$(cr) calculated from the present model are in good agreement with the NBS value [93] and that given by Song and Yao [94], but slightly differ from the value derived from the $\ln K$ reported by Kwok et al. [95]. This may result from the inaccurate representation of the component activity of the extended UNIQUAC model reported by Kwok et al. [95] for the binary system $Li_2SO_4 + H_2O$. The deviation of standard enthalpy $\Delta_f H_m^{\ominus}$ of $Li_2SO_4·H_2O$ (cr) between the present model values and the NBS value is about 1%, which is usually reasonable. However, the small difference of $\Delta_f H_m^{\ominus}$ will result in significant deviation on the standard entropy $S_m^{\ominus}$ of $Li_2SO_4·H_2O$ (cr), as shown in Table 5, due to the compensation effect between $\Delta_f H_m^{\ominus}$ and $S_m^{\ominus}$. The heat capacity $C_{p,m}$ of $Li_2SO_4·H_2O$(cr) estimated from the group contribution of crystal water is slightly larger than that listed in the NBS table.

The standard Gibbs energy $\Delta_f G_m^{\ominus}$ of $Na_2SO_4·10H_2O$(cr) calculated from the present model are in good agreement with the NBS value, the value given by Pabalan and Pitzer [11] and the value calculated from the $\ln K$ reported by Steiger et al. [9] and the standard Gibbs energy of ion species and water calculated from the HKF equation of state. Other standard thermodynamic quantities of $Na_2SO_4·10H_2O$(cr) from different sources agree with each other, except for the $\Delta_f H_m^{\ominus}$ reported by Pabalan and Pitzer [11], which is obviously deviated from other values and incorrect. The standard thermodynamic quantities of metastable phase $Na_2SO_4·7H_2O$(cr) derived from the present model are reported here without any comparison. The standard thermodynamic quantities of Na_2SO_4(cr) from different sources are in good agreement and their reliability can be ascertained.

The standard thermodynamic quantities $\Delta_f G_m^{\ominus}$ and $\Delta_f H_m^{\ominus}$ of solid phase K_2SO_4(cr) obtained in this study agree with these reported by Pabalan and Pitzer [11] well, but differ significantly (about 8.0 kJ mol^{-1}) from the $\Delta_f H_m^{\ominus}$ values given by NBS table. Hence, we suppose the thermodynamic values of K_2SO_4(cr) derived from solubility

Fig. 21. Specific heat capacity c_p of Na_2SO_4(aq) solution at various temperatures and molalities. Symbols: experimental data reported in literature [54]; Lines: the present model results.

Fig. 22. Specific heat capacity c_p of K$_2$SO$_4$(aq) solution at various temperatures and molalities. Symbols: experimental data reported in literature [53,65]; Lines: the present model results.

data by Pabalan and Pitzer [11] and these determined in the present study are recommended.

To determine the relative stability of magnesium sulfate hydrates at complex temperature and humidity conditions accurately, extensive papers [11,12,71,89,90,93,96] have been published aiming to obtain reliable standard thermodynamic quantities of these compounds. From

the present model of MgSO$_4$ + H$_2$O system, these thermodynamic quantities were determined here independent from those reported in other literature. These values are listed in Table 5. The standard Gibbs energy $\Delta_f G_m^\Theta$ of MgSO$_4$·11H$_2$O(cr) obtained in the present study agrees with that of Steiger et al. [12] well, but the difference of $\Delta_f H_m^\Theta$ between the present value and that reported by Chou and Seal II [89] is
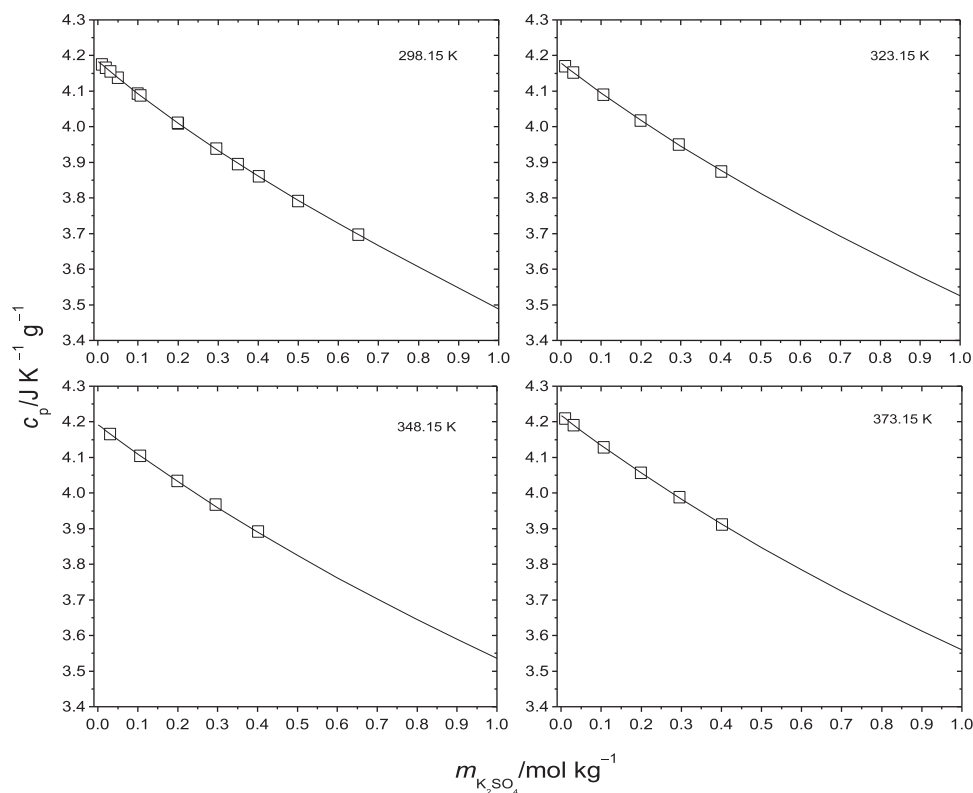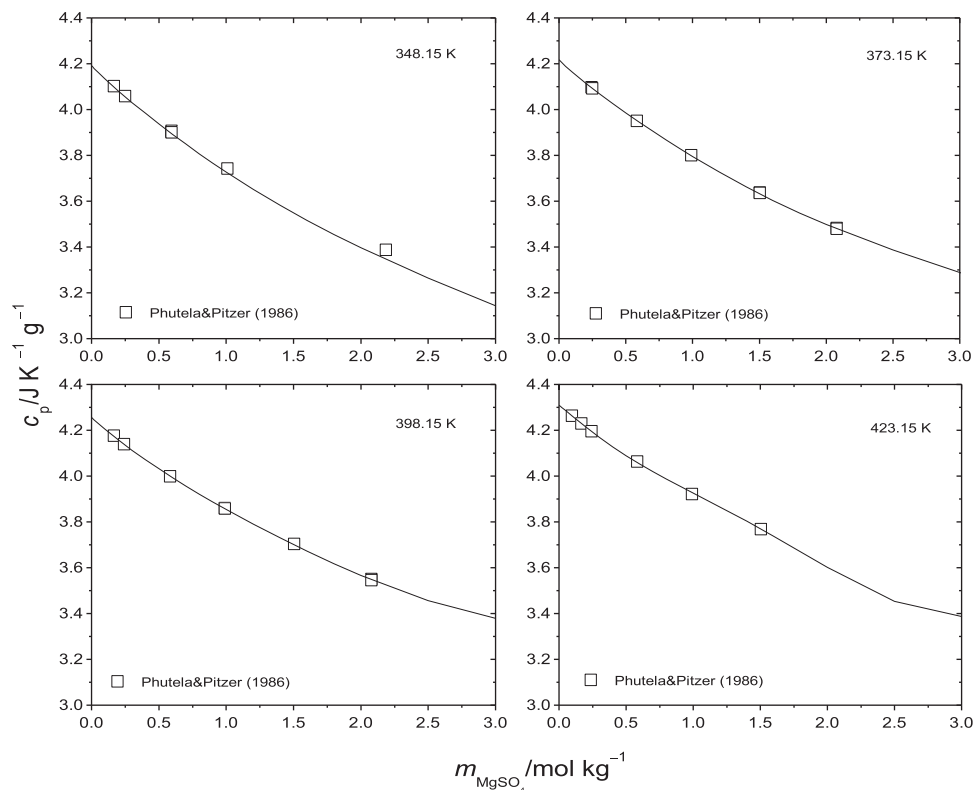

Fig. 23. Specific heat capacity c_p of MgSO$_4$(aq) solution at various temperatures and molalities. Symbols: experimental data reported in literature [75]; Lines: the present model results.

Table 5

Standard state thermodynamic values of solid phases at $T = 298.15$ K.

Solids	$\Delta_f G_m^{\ominus}$ (kJ mol^{-1})	$\Delta_f H_m^{\ominus}$ (kJ mol^{-1})	$S_m^{\ominus}$ (J mol^{-1} K^{-1})	$C_{p,m}$ (J mol^{-1} K^{-1})	Reference
Li$_2$SO$_4$·H$_2$O(cr)	−1564.32	−1733.64	141.69	161.09	This work
	−1565.50	−1715.52	163.60	151.08	[93]
	−1564.41	–	–	–	[94]
	−1560.53	–	–	–	[95]
Na$_2$SO$_4$·10H$_2$O(cr)	−3646.55	−4326.85	583.69	563.14	This work
	−3646.56	–	–	–	[9]
	−3646.71	−3658.12	592.04	574.39	[11]
	−3646.85	−4327.26	592.00	–	[93]
Na$_2$SO$_4$·7H$_2$O(cr)	−2931.10	−3435.81	472.86	388.00	This work
Na$_2$SO$_4$(cr,V)	−1270.02	−1388.32	136.09	128.14	This work
	−1269.97	–	–	–	[9]
	−1270.12	−1387.02	149.57	127.79	[11]
	−1270.16	−1387.08	149.58	128.20	[93]
K$_2$SO$_4$(cr)	−1319.74	−1438.02	174.77	131.34	This work
	−1319.70	−1437.74	175.59	131.07	[11]
	−1321.37	−1427.27	175.56	131.46	[93]
MgSO$_4$·11H$_2$O(cr)	−3815.31	−4565.84	523.27	574.88	This work
	−3815.24	–	–	–	[12]
	–	−4579.79	–	–	[89]
MgSO$_4$·7H$_2$O(cr)	−2868.98	−3390.49	358.42	400.88	This work
	−2869.83	−3386.74	372.38	390.60	[11]
	−2868.91	–	–	–	[12]
	−2868.96	–	364.83	–	[71]
	−2869.37	–	364.83	–	[71]
	−2871.00	−3388.70	371.30	–	[90]
	−2871.50	−3388.71	372.00	–	[93]
	–	−3389.04	372.38	–	[96]
MgSO$_4$·6H$_2$O(cr)	−2630.30	−3087.42	341.10	357.38	This work
	−2630.03	−3085.61	348.11	348.42	[11]
	−2630.15	–	–	–	[12]
	−2630.36	–	344.02	–	[71]
	−2630.18	–	344.31	–	[71]
	−2632.30	−3087.30	348.50	–	[90]
	−2631.80	−3087.00	348.10	348.11	[93]
	–	−3087.29	348.11	–	[96]
MgSO$_4$·5H$_2$O(cr)	−2390.92	−2790.92	299.44	313.88	This work
	−2392.38	–	296.81	306.16	[11]
	−2389.48	–	–	–	[12]
MgSO$_4$·4H$_2$O(cr)	−2151.71	−2497.98	246.39	270.38	This work
	−2152.98	−2496.49	254.74	263.48	[11]
	−2151.49	–	–	–	[12]
	−2153.80	−2496.10	259.90	–	[90]
	–	−2498.70	254.48	261.06	[90]
	–	−2496.60			[93]
	–	−2497.01	246.86	–	[96]
MgSO$_4$·H$_2$O(cr)	−1435.56	−1614.01	109.51	139.88	This work
	−1435.68	−1609.60	124.63	134.25	[11]
	−1435.75	–	–	–	[12]
	−1437.90	−1611.50	126.00	–	[90]
	−1428.70	−1602.10	126.40	–	[93]
	–	−1610.00	124.36	–	[96]
CaSO$_4$·2H$_2$O(cr)	−1797.62	−2032.44	162.55	188.12	This work
	−1797.28	−2022.63	194.10	186.02	[93]
CaSO$_4$·1/2H$_2$O(cr)	−1437.73	−1585.68	104.01	122.87	This work
	−1436.74	−1576.74	130.50	119.41	[93]
CaSO$_4$(cr)	−1322.47	−1444.0	76.02	101.12	This work
	−1321.79	−1434.11	106.7	99.66	[93]

relatively large. It is hard to evaluate which one is more reliable due to the lack of other independent proofs. The present study just gives one set of standard thermodynamic quantities of MgSO$_4$·11H$_2$O(cr) for reference. The standard thermodynamic quantities of MgSO$_4$·7H$_2$O(cr), MgSO$_4$·6H$_2$O(cr), MgSO$_4$·5H$_2$O(cr) and MgSO$_4$·4H$_2$O(cr) from different sources are in good agreement and their reliability can be ascertained. The standard Gibbs energy $\Delta_f G_m^{\ominus}$ of MgSO$_4$·H$_2$O(cr) in the present study agrees with most literature values except for that of NBS table, which should be corrected in further. The standard entropy $S_m^{\ominus}$ of MgSO$_4$·H$_2$O (cr) of this work is significantly smaller than other values and the reliability of the present value may be questionable. At the same time, the $\Delta_f H_m^{\ominus}$ of MgSO$_4$·H$_2$O(cr) determined in this work is also smaller than other values, and the small $S_m^{\ominus}$ values of this work results from the

compensation effect between $\Delta_f H_m^{\ominus}$ and $S_m^{\ominus}$.

Except for MgSO$_4$·H$_2$O(cr), the small $\Delta_f H_m^{\ominus}$ and $S_m^{\ominus}$ values are also exhibited for all calcium sulfate hydrates compared with other literature values. This phenomenon probably results from the improper nonzero parameter selection in regression. Nevertheless, the reliability of the standard Gibbs energies $\Delta_f G_m^{\ominus}$ of calcium sulfate minerals determined in the present study can be assured.

5. Conclusions

The phase equilibria and thermodynamic properties of five binary sulfate systems Li$_2$SO$_4$ + H$_2$O, Na$_2$SO$_4$ + H$_2$O, K$_2$SO$_4$ + H$_2$O, MgSO$_4$ + H$_2$O and CaSO$_4$ + H$_2$O were simulated using the PSC excess

Gibbs energy model under a comprehensive thermodynamic framework. Various type of thermodynamic properties (i.e., water activity, osmotic coefficient, mean ionic activity coefficient, enthalpy of dilution and solution, relative apparent molar enthalpy, heat capacity of aqueous phase and solid phases) were collected and applied to regress these model parameters. Comparisons of the present model values with previously reported experimental or model values in literature indicate that the temperature dependent model parameters determined in this study can describe all of the thermodynamic and phase equilibria properties of these binary systems over wide temperature (from freezing point to approx. 500 K) and concentration (from infinite dilution to saturation) ranges with one set parameters. The present thermodynamic models for these binary sulfate systems together with our previous reported models for binary chloride systems provide a basis for the prediction of comprehensive properties of multi-component salt lake brine systems at various temperature and concentration conditions.

Acknowledgments

Appendix A. Supporting information

Supplementary data associated with this article can be found in the online version at http://dx.doi.org/10.1016/j.calphad.2018.01.002.

References

[1] D. Li, D. Zeng, H. Han, L. Guo, X. Yin, Y. Yao, Phase diagrams and thermochemical modeling of salt lake brine systems. I. $LiCl + H_2O$ system, CALPHAD 51 (2015) 1–12.

[2] D. Li, D. Zeng, X. Yin, H. Han, L. Guo, Y. Yao, Phase diagrams and thermochemical modeling of salt lake brine systems. II. $NaCl + H_2O$, $KCl + H_2O$, $MgCl_2 + H_2O$ and $CaCl_2 + H_2O$ systems, CALPHAD 53 (2016) 78–89.

[3] S.L. Clegg, K.S. Pitzer, Thermodynamics of multicomponent, miscible, ionic solutions: generalized equations for symmetrical electrolytes, J. Phys. Chem. 96 (1992) 3513–3520.

[4] S.L. Clegg, S.S. Ho, C.K. Chan, P. Brimblecombe, Thermodynamic properties of aqueous $(NH_4)_2SO_4$ to high supersaturation as a function of temperature, J. Chem. Eng. Data 40 (1995) 1079–1090.

[5] D. Rowland, Thermodynamically-robust Pitzer equations for volumetric properties of electrolyte solutions, Talanta 144 (2015) 90–92.

[6] A. Lach, F. Boulahya, L. André, A. Lassin, M. Azaroual, J.-P. Serin, P. Cézac, Thermal and volumetric properties of complex aqueous electrolyte solutions using the Pitzer formalism – The PhreeSCALE code, Comput. Geosci. 92 (2016) 58–69.

[7] H.F. Holmes, R.E. Mesmer, Thermodynamics of aqueous solutions of the alkali metal sulfates, J. Solut. Chem. 15 (1986) 495–517.

[8] H.F. Holmes, R.E. Mesmer, Isopiestic studies of aqueous solutions at elevated temperatures VIII. The alkali-metal sulfates, J. Chem. Thermodyn. 18 (1986) 263–275.

[9] M. Steiger, J. Kiekbusch, A. Nicolai, An improved model incorporating Pitzer's equations for calculation of thermodynamic properties of pore solutions implemented into an efficient program code, Constr. Build. Mater. 22 (2008) 1841–1850.

[10] D.A. Palmer, D.G. Archer, J.A. Rard, Isopiestic determination of the osmotic and activity coefficients of $K_2SO_4(aq)$ at the temperatures 298.15 and 323.15 K, and revision of the thermodynamic properties of the $K_2SO_4 + H_2O$ system, J. Chem. Eng. Data 47 (2002) 1425–1431.

[11] R.T. Pabalan, K.S. Pitzer, Thermodynamics of concentrated electrolyte mixtures and the prediction of mineral solubilities to high temperatures for mixtures in the system Na-K-Mg-Cl-SO$_4$-OH-H$_2$O, Geochim. Cosmochim. Acta 51 (1987) 2429–2443.

[12] M. Steiger, K. Linnow, D. Ehrhardt, M. Rohde, Decomposition reactions of magnesium sulfate hydrates and phase equilibria in the $MgSO_4 - H_2O$ and $Na^+ - Mg^{2+} - Cl^- - SO_4^{2-} - H_2O$ systems with implications for Mars, Geochim. Cosmochim. Acta 75 (2011) 3600–3626.

[13] P.M. Mathias, M. Mendez, Simulation of phosphoric acid production by the dihydrate process, 22nd Clearwater Convention on Phosphate Fertilizer & Sulfuric Acid Technology, Florida.

[14] Y. Peng, Z. Zhu, R.D. Braatz, A.S. Myerson, Gypsum crystallization during phosphoric acid production: modeling and experiments using the mixed-solvent-electrolyte thermodynamic model, Ind. Eng. Chem. Res. 54 (2015) 7914–7924.

[15] W. Wang, D. Zeng, Q. Chen, X. Yin, Experimental determination and modeling of gypsum and insoluble anhydrite solubility in the system $CaSO_4 - H_2SO_4 - H_2O$, Chem. Eng. Sci. 101 (2013) 120–129.

[16] H.C. Helgeson, D.H. Kirkham, G.C. Flowers, Theoretical prediction of the thermodynamic behavior of aqueous electrolytes at high pressure and temperatures: IV. Calculation of activity coefficients, osmotic coefficients, and apparent molal and standard and relative partial molal properties to 600 °C and 5 kbar, Am. J. Sci. 28 (1981) 1249–1516.

[17] E.L. Shock, H.C. Helgeson, Calculation of thermodynamic and transport properties of aqueous species at high pressures and temperatures: correlation algorithms for ionic species and equation of state predictions to 5 kbar and 1000 °C, Geochim. Cosmochim. Acta 52 (1988) 2009–2036.

[18] J.M. Dick, Calculation of the relative metastabilities of proteins using the CHNOSZ software package, Geochem. Trans. 9 (2008) 1–17.

[19] H.Y. Afeefy, J.F. Liebman, S.E. Stein, "Neutral Thermochemical Data" in NIST Chemistry WebBook, NIST Standard Reference Database Number 69, Eds. P.J. Linstrom and W.G. Mallard, National Institute of Standards and Technology, Gaithersburg MD, 20899, ⟨http://webbook.nist.gov⟩, (retrieved September 23.

[20] D.G. Archer, Thermodynamic properties of the $NaCl + H_2O$ system. II. thermodynamic properties of NaCl(aq), NaCl·2H$_2$O(cr) and phase equilibria, J. Phys. Chem. Ref. Data 21 (4) (1992) 793–829.

[21] R.A. Robinson, J.M. Wilson, R.H. Stokes, The activity coefficients of lithium, sodium and potassium sulfate and sodium thiosulfate at 25° from isopiestic vapor pressure measurements, J. Am. Chem. Soc. 63 (1941) 1011–1013.

[22] J.A. Rard, S.L. Clegg, D.A. Palmer, Isopiestic determination of the osmotic and activity coefficients of $Li_2SO_4(aq)$ at $T = 298.15$ and 323.15 K, and representation with an extended ion-interaction (Pitzer) model, J. Solut. Chem. 36 (2007) 1347–1371.

[23] F.F. Li, Y. Yao, Isopiestic studies of thermodynamics properties in $LiCl - Li_2SO_4 - H_2O$ system at 273.15 K, Chem. Res. Appl. 16 (2004) 33–36 (in Chinese).

[24] F.F. Li, Y. Yao, Isopiestic studies of thermodynamics properties in $LiCl - Li_2SO_4 - H_2O$ system at 323.15 K, J. Salt Lake Res. 12 (2004) 37–42 (in Chinese).

[25] J. Baabor S, M.A. Gilchrist, E.J. Delgado, Osmotic and activity coefficients of aqueous lithium sulfate solutions at 40 °C, J. Solut. Chem. 25 (1996) 1105–1111.

[26] V.K. Filippov, A.M. Kalinkin, S.K. Vasin, Thermodynamics of phase equilibria of aqueous (lithium sulfate + alkali-metal sulfate) (alkali metal: Na, K, and Rb), and (sodium sulfate + rubidium sulfate), at 298.15 K using Pitzer's model, J. Chem. Thermodyn. 21 (1989) 935–946.

[27] W.H. Leung, F.J. Millero, The enthalpy of formation of magnesium sulfate ion pairs, J. Solut. Chem. 4 (1975) 145–159.

[28] P.T. Thompson, D.E. Smith, R.H. Wood, Enthalpy of dilution of aqueous Na_2SO_4 and Li_2SO_4, J. Chem. Eng. Data 19 (1974) 386–388.

[29] E. Lange, H. Streeck, Verdünnungswärmen einiger 2-1-wertiger bzw. 1-2-wertiger Salze in großer Verdünnung bei 25 °C. II. $Mg(NO_3)_2$, $Ca(NO_3)_2$, $Sr(NO_3)_2$, $Ba(NO_3)_2$, Li_2SO_4, Na_2SO_4, K_2SO_4, Rb_2SO_4, Cs_2SO_4, einschließlich einiger neuerer Messungen am $MgSO_4$ und $CaSO_4$, Z. Phys. Chem. 157 (1931) 1–31.

[30] A.N. Campbell, The system $Li_2SO_4 - H_2O$, J. Am. Chem. Soc. 65 (1943) 2268–2271.

[31] M.P. Applebey, F.H. Crawford, K. Gordon, Vapor pressures of saturated solution lithium chloride and lithium sulfate, J. Chem. Soc. 2 (1934) 1665–1671.

[32] S.P. Xia, H.Q. Pan, S.Y. Gao, The solubility of ternary system $Li_2SO_4 - C_2H_5OH - H_2O$ at -20 °C to $+50$ °C, Chin. J. Appl. Chem. 5 (1988) 82–84 (in Chinese).

[33] A. Carton, F. Sobron, S. Bolado, Composition and density of saturated solutions of lithium sulfate + water + ethanol, J. Chem. Eng. Data 39 (1994) 61–62.

[34] B. Li, Q.Z. Wang, J. Li, C.H. Fang, P.S. Song, A study on the ternary system $Li^+, K^+/SO_4^{2-} - H_2O$ and $Li^+, Mg^{2+}/SO_4^{2-} - H_2O$ at 25 °C, Acta Phys. -Chim. 10 (1994) 536–542 (in Chinese).

[35] G. Aravamudan, System $Li_2SO_4 - MgSO_4 - H_2O$ at 30 °C, Can. J. Chem. 40 (1962) 1035–1037.

[36] L. Gemlin, Gmelins Handbuch Der Anorganischen Chemie: 20: Lithium, Verlag Chemie, GMBH. (in Germany), 1960.

[37] V.E. Plyushchev, V.B. Tulinova, Issledovanie sistemy $LiCl - Li_2SO_4 - H_2O$, Zh. Neorg. Khim. 4 (1959) 1184–1189 (in Russian).

[38] K.Y. Khu, Politerma rastvorimosti V system $Li_2SO_4 - Na_2SO_4 - H_2O$, Zh. Neorg. Khim. 4 (1959) 1910–1918 (in Russian).

[39] W.F. Linke, A. Seidell, Solubilities: Inorganic and Meta-Organic Compounds, 4th ed., American Chemical Society, Washington, DC, 1965.

[40] R.F. Platford, Osmotic coefficients of aqueous solutions of seven compounds at 0°, J. Chem. Eng. Data 18 (2) (1973) 215–217.

[41] J.A. Rard, S.L. Clegg, D.A. Palmer, Isopiestic determination of the osmotic coefficients of $Na_2SO_4(aq)$ at 25 and 50 °C, and representation with ion-interaction (Pitzer) and model fraction thermodynamic models, J. Solut. Chem. 29 (2000) 1–49.

[42] O.N. Bhatnagar, A.N. Campbell, Osmotic and activity coefficients of sodium sulphate in water from 50 to 150 °C, Can. J. Chem. 59 (1981) 123–126.

[43] K.L. Hellams, C.S. Patterson, B.H. Prentice III, M.J. Taylor, Osmotic properties of some aqueous solutions at 45 °C, J. Chem. Eng. Data 10 (1965) 323–325.

[44] W.T. Humphries, C.F. Kohrt, C.S. Patterson, Osmotic properties of some aqueous electrolytes at 60 °C, J. Chem. Eng. Data 13 (1968) 327–330.

[45] J.T. Moore, W.T. Humphries, C.S. Patterson, Isopiestic studies of some aqueous

electrolyte solutions at 80 °C, J. Chem. Eng. Data 17 (1972) 180–182.

[46] C.S. Patterson, L.O. Gilpatrick, B.A. Soldano, The osmotic behavior of representative aqueous salt solutions at 100 °C, J. Chem. Soc. (1960) 2730–2734.

[47] W. Kangro, A. Groeneveld, Konzentrierte wäßrige Lösungen, I, Z. Phys. Chem. Neue Folge 32 (1962) 110–126.

[48] R.N. Goldberg, Evaluated activity of osmotic coefficients for aqueous solutions: thirty-six uni-bivalent electrolytes, J. Phys. Chem. Ref. Data 10 (3) (1981) 671–764.

[49] Y. Yao, G. Atkinson, Activity coefficients in aqueous $Na_2SO_4 - CuSO_4$ at 25 °C, Acta Phys. -Chim. 7 (1) (1991) 57–63 (in Chinese).

[50] H.P. Snipes, C. Manly, D.D. Ensor, Heats of dilution of aqueous electrolytes: temperature dependence, J. Chem. Eng. Data 20 (3) (1975) 287–291.

[51] J.E. Mayrath, R.H. Wood, Enthalpy of dilution of aqueous solutions of Na_2SO_4, K_2SO_4, and $MgSO_4$, at 373.15 K and 423.65 K and of $MgCl_2$ at 373.15, 423.65, and 472.95 K, J. Chem. Eng. Data 28 (1) (1983) 56–59.

[52] J.C. Li, Z.X. Zhai, Z.M. Zeng, L.Y. Wang, Enthalpies of dilution and relative apparent molal enthalpies of the major aqueous salts of salt lakes at 298.15 K, Acta Phys. -Chim. 10 (8) (1994) 759–764 (in Chinese).

[53] M. Randall, F.D. Rossini, Heat capacities in aqueous salt solutions, J. Am. Chem. Soc. 51 (2) (1929) 323–345.

[54] P.S.Z. Rogers, K.S. Pitzer, High-temperature, thermodynamic properties of aqueous sodium sulfate solutions, J. Phys. Chem. 85 (1981) 2886–2895.

[55] M. Randall, C.N. Scott, The freezing point and activity coefficients of aqueous barium nitrate, sodium sulfate and sulfuric acid, J. Am. Chem. Soc. 49 (3) (1927) 647–656.

[56] L.C. De Coppet, Reserchessur la surfusion et la sursaturation, Ann. Chim. Phys. 8 (10) (1907) 457–527.

[57] H. Hartley, B.M. Jones, G.A. Hutchinson, The spontaneous crystallization of sodium sulphate solutions, J. Chem. Soc. Trans. 93 (1908) 825–883.

[58] U. Sborgi, E. Bovalini, Gazz. Chim. Ital. 54 (1924) 919–933.

[59] R.E. Vener, A.R. Thompson, Solubility and density isotherms for sodium sulfate-ethylene glycol-water, Ind. Eng. Chem. 41 (10) (1949) 2242–2247.

[60] E. Berkeley, On some physical constants of saturated solutions, Philos. Trans. R. Soc. A 203 (1904) 189–215.

[61] T.W. Richards, V. Yngve, The solubility of sodium sulfate as a means of determining temperatures, J. Am. Chem. Soc. 40 (1) (1918) 164–174.

[62] R.D. Eddy, A.W.C. Menzies, The solubilities of certain inorganic compounds in ordinary water and in deuterium water, J. Phys. Chem. 44 (1940) 207–235.

[63] O.C. Okorafor, Solubility and density isotherms for the sodium sulfate-water-methanol system, J. Chem. Eng. Data 44 (1999) 488–490.

[64] F. Malatesta, L. Carbonaro, N. Fanelli, S. Ferrini, A. Giacomelli, J. Solut. Chem. 28 (5) (1999) 593–619.

[65] P.P.S. Saluja, R.J. Lemire, J.C. LeBlanc, High-temperature thermodynamics of aqueous alkali-metal salts, J. Chem. Thermodyn. 24 (2) (1992) 181–203.

[66] J. Eysseltová, R. Bouaziz, IUPAC-NIST solubility data series 93. Potassium sulfate in water, J. Phys. Chem. Ref. Data 41 (1) (2012) 1–48.

[67] J. Zhang, D.D. Li, Y. Yao, B. Sun, D. Zeng, P.S. Song, Thermodynamic properties of $LiCl + MgSO_4 + H_2O$ at temperatures from 273.15 K to 373.15 K and representation with Pitzer ion-interaction model, J. Chem. Eng. Data 61 (2016) 2277–2291.

[68] C.W. Childs, R.F. Platford, Excess free energies of mixing at temperatures below 25 °C. Isopiestic measurements on the systems $H_2O - NaCl - Na_2SO_4$ and $H_2O - NaCl - MgSO_4$, Aust. J. Chem. 24 (1971) 2487–2491.

[69] J.A. Rard, D.G. Miller, Isopiestic determination of the osmotic coefficients of aqueous Na_2SO_4, $MgSO_4$, and $Na_2SO_4 - MgSO_4$, J. Chem. Eng. Data 26 (1) (1981) 33–38.

[70] R.A. Robinson, R.S. Jones, The activity coefficients of some bivalent metal sulfates in aqueous solution from vapor pressure measurements, J. Am. Chem. Soc. 58 (6) (1936) 959–961.

[71] D.G. Archer, J.A. Rard, Isopiestic investigation of the osmotic and activity coefficients of aqueous $MgSO_4$ and the solubility of $MgSO_4·7H_2O(cr)$ at 298.15 K: thermodynamic properties of the $MgSO_4 + H_2O$ system to 440 K, J. Chem. Eng. Data 43 (1998) 791–806.

[72] F. Kuschel, J. Seldel, Osmotic and activity coefficients of aqueous $K_2SO_4 - MgSO_4$ and $KCl - MgCl_2$ at 25 °C, J. Chem. Eng. Data 30 (1985) 440–445.

[73] H.F. Holmes, R.E. Mesmer, Isopiestic studies of aqueous solutions at elevated temperatures VII. $MgSO_4$ and $NiSO_4$, J. Chem. Thermodyn. 15 (1983) 709–719.

[74] H. Yokoyama, H. Yamatera, Ion association of some 2:2 electrolytes in water at 25 °C. I. Studies of magnesium, calcium, manganese, and tris(1,10-phenanthroline)-ruthenium(II) sulfate solutions with a vapor-pressure osmometer, B. Chem. Soc. Jpn. 48 (10) (1975) 2708–2718.

[75] R.C. Phutela, K.S. Pitzer, Heat capacity and other thermodynamic properties of aqueous magnesium sulfate to 473 K, J. Phys. Chem. 90 (1986) 895–901.

[76] V. Pillay, R.S. Cärtner, C. Himawan, M.M. Seckler, A.E. Lewis, G.-J. Witkamp, $MgSO_4 + H_2O$ system at eutectic conditions and thermodynamic solubility products of $MgSO_4·12H_2O(s)$ and $MgSO_4·7H_2O(s)$, J. Chem. Eng. Data 50 (2005) 551–555.

[77] L. Gemlin, Magnetische und Elektrische Eigenschaften des Eisens und Seiner Legierungen, Springer, 1937.

[78] H.H. Ting, W.L. McCabe, Solubility of magnesium sulfate heptahydrate, Ind. Eng. Chem. 26 (11) (1934) 1027–1028.

[79] H.L. Robson, The system $MgSO_4 - H_2O$ from 68 to 240 °C, J. Am. Chem. Soc. 49 (11) (1927) 2772–2783.

[80] A. Smits, J. Rinse, L.H. Louwe Kooymans, Das system wasser-magnesium sulfate, Z. Phys. Chem. 135 (1928) 78–84.

[81] T.H. Lilley, C.C. Briggs, Activity coefficients of calcium sulphate in water at 25 °C, Proc. R. Soc. Lond. A 349 (1976) 355–368.

[82] J. Block, O.B. Waters Jr., The $CaSO_4 - Na_2SO_4 - NaCl - H_2O$ system at 25 to 100 °C, J. Chem. Eng. Data 13 (1968) 336–344.

[83] E. AN Zen, Solubility measurements in the system $CaSO_4 - NaCl - H_2O$ at 35, 50, and 70 °C and one atmosphere pressure, J. Petrol. 6 (1965) 124–164.

[84] A.E. Hill, The transition temperature of gypsum to anhydrite, J. Am. Chem. Soc. 59 (11) (1937) 2242–2244.

[85] E.P. Partridge, A.H. White, The solubility of calcium sulfate from 0 to 200 °C, J. Am. Chem. Soc. 51 (2) (1929) 360–370.

[86] W.L. Mashall, R. Slusher, Aqueous systems at high temperature. Solubility to 200.degree. of calcium sulfate and its hydrates in sea water and saline water concentrates, and temperature-concentration limits, J. Chem. Eng. Data 13 (1) (1968) 83–93.

[87] J. Sohr, W. Voigt, D. Zeng, IUPAC-NIST solubility data series. 104. Lithium sulfate and its double salts in aqueous solution, J. Phys. Chem. Ref. Data 46 (2017) 023101.

[88] G.M. Marion, R.E. Farren, Mineral solubilities in the Na-K-Mg-Ca-Cl-SO_4-H_2O systems: a re-evaluation of the sulfate chemistry in the Spencer-Moller-Weare model, Geochim. Cosmochim. Acta 63 (9) (1999) 1305–1318.

[89] I.M. Chou, R.R. Seal II, Magnesium and calcium sulfate stabilities and the water budget of Mars, J. Geophys. Res. 112 (2007) (E11004 1-10).

[90] K.D. Grevel, J. Majzlan, Internally consistent thermodynamic data for magnesium sulfate hydrates, Geochim. Cosmochim. Acta 73 (2009) 6805–6815.

[91] A. Apelblat, Enthalpy of solution of lithium sulfate and lithium sulfate monohydrate in water at 298.15 K, J. Chem. Thermodyn. 17 (1985) 769–773.

[92] B. Hu, L. Hnědkovský, G. Hefter, Heat capacities of aqueous solutions of lithium sulfate, lithium perchlorate, and lithium trifluoromethanesulfonate at 298.15 K, J. Chem. Eng. Data 61 (2016) 2149–2154.

[93] D.D. Wagman, W.H. Evans, V.B. Parker, R.H. Schumm, I. Halow, S.M. Bailey, K.L. Churney, R.L. Nuttall, The NBS tables of chemical thermodynamic properties. Selected values for inorganic and C1 and C2 organic substances in SI units, J. Phys. Chem. Ref. Data 11 (1982) 1–392.

[94] P.S. Song, Y. Yao, Thermodynamics of phase diagram of the salt lake brine system at 298.15 K V. Model for the system Li^+, Na^+, K^+, Mg^{2+}/Cl^-, $SO_4^{2-} - H_2O$ and its applications, CALPHAD 27 (2003) 343–352.

[95] K.S. Kowk, K.N. Ng, M.E. Taboada, L.A. Cisternas, Thermodynamics of salt lake system: representation, experiments, and visualization, AIChE J. 54 (3) (2008) 706–727.

[96] C.W. DeKock, Thermodynamic properties of selected metal sulfates and their hydrates, U.S. Bur. Mines Inf. Circ. 9081 (1986) 59.